



# Differential regulation of human monocytes and NK cells by antibody-opsionized tumors

Jun Yin<sup>1</sup> · Alex J. Albers<sup>1</sup> · Thomas S. Smith<sup>1,2</sup> · Geoffrey T. Riddell<sup>1</sup> · John O. Richards<sup>1</sup> 

Received: 31 May 2017 / Accepted: 28 May 2018 / Published online: 31 May 2018  
© Springer-Verlag GmbH Germany, part of Springer Nature 2018

## Abstract

The monocyte network is important for therapeutic efficacy of antibody therapies against cancer. One mechanism which monocytes/macrophages use to kill cancer cells is phagocytosis. Using trastuzumab and human breast cancer cell lines as a model, we used flow cytometry to evaluate the importance of avidity, antigen density, Fcγ receptor (FcγR) expression, and FcγR polymorphisms in human monocyte phagocytosis. By increasing avidity for the tumor through the addition of pertuzumab to trastuzumab, there was a two-to-threefold increase in phagocytosis potency against the HCC1419 cell line compared to antibodies alone, while NK cell-mediated antibody-dependent cellular cytotoxicity (ADCC) failed to increase tumor cell death. Consistent with increasing the avidity through multiple antibodies, antigen density significantly enhanced phagocytosis with breast cancer cell lines that were HER2 gene-amplified compared to non-amplified tumor cells. Confirmation that high antigen density enhanced phagocytosis was obtained when HER2 was overexpressed in HER2 non-amplified cell lines. In contrast, NK cell ADCC failed to distinguish differences in tumor cell death when comparing gene-amplified and non-amplified breast cancer cell lines. The level of phagocytosis was influenced by FcγRIIa and FcγRIIIa expression. Most monocytes are FcγRIIIa<sup>-</sup>, and the induction of the receptor significantly enhances antibody-dependent phagocytosis. Although both receptors are involved, when blocked FcγRIIIa had a greater influence on phagocytosis. Furthermore, the polymorphism FcγRIIIa 158V significantly enhanced phagocytosis; whereas FcγRIIa 131H polymorphism appeared to improve phagocytosis but was not statistically significant. Targeting of monocytes for enhanced phagocytosis may improve the effectiveness of therapeutic antibodies to improve clinical outcomes.

**Keywords** Antibody-dependent cellular cytotoxicity (ADCC) · Antibody-dependent cellular phagocytosis (ADCP) · Monocyte/macrophages · NK cells · HER2 · Breast cancer

## Abbreviations

ADCC Antibody-dependent cellular cytotoxicity  
AF Alexa fluor  
CFSE Carboxyfluorescein succinimidyl ester  
EpCAM Epithelial cell adhesion molecule

ErbB-2 Erb-b2 receptor tyrosine kinase 2  
F Phenylalanine  
FcγRs Fcγ receptors  
H Histidine  
HER2 Human epidermal growth factor receptor 2  
PBMC Peripheral blood mononuclear cell  
R Arginine  
V Valene

**Electronic supplementary material** The online version of this article (<https://doi.org/10.1007/s00262-018-2179-z>) contains supplementary material, which is available to authorized users.

✉ Jun Yin  
jun.yin@aurora.org

✉ John O. Richards  
gimrich2000@yahoo.com

<sup>1</sup> Aurora Research Institute, Aurora Health Care, 960 N. 12th Street, 3rd floor, Milwaukee, WI 53233, USA

<sup>2</sup> Computer Science, University of Wisconsin Milwaukee, Milwaukee, WI, USA

## Introduction

Antibody-dependent cellular cytotoxicity (ADCC) is a key effector mechanism for tumor-targeting antibodies [1]. NK cell-mediated ADCC has shown that antigen density, affinity for antigen, affinity for Fc, and FcγR density influence NK cell-mediated ADCC [2–6], but the relevance of NK cell-mediated ADCC in vivo has been questioned [7, 8].

Scheuer et al. demonstrated that the addition of pertuzumab to trastuzumab had no effect on NK cell-mediated ADCC compared to trastuzumab alone, *in vitro* [9]. In a mouse model, the combination of pertuzumab and trastuzumab significantly reduced tumor growth compared to the individual antibodies [9]. Furthermore, the combination of pertuzumab, trastuzumab, and docetaxel in the clinic significantly improved overall survival in metastatic breast cancer compared to trastuzumab and docetaxel [10, 11]. In a syngeneic tumor model, NK cells and CD8 T cells were deemed necessary for antibody-mediated tumor rejection that targeted rat erb-b2 receptor tyrosine kinase 2 (ErbB-2) [12]. Surprisingly, mice deficient in perforin were equally capable of tumor rejection using anti-ErbB-2, which indicated that lymphocyte cytotoxicity was not necessary [12] and suggests other mechanisms of action for NK cells with antibody therapies.

Multiple studies implicate the monocyte network as effector cells for antibody therapeutics. Specific Fc $\gamma$  receptors (Fc $\gamma$ R) or common  $\gamma$ -chain knockout mice support NK cells and the monocyte network in antibody-mediated effector function against tumors [13, 14]. Depletion of the inhibitory receptor Fc $\gamma$ RII, which is not expressed on NK cells, enhanced tumor rejection in mice and suggests a role of monocytes [13]. Clodronate depletion of monocytes was found to inhibit B-cell depletion and antibody-mediated tumor rejection in multiple tumor models, implying that monocytes are involved in antibody-mediated cellular depletion or tumor rejection, respectively [14, 15]. In the clinic, objective response rates and progression-free survival with trastuzumab were significantly correlated with the Fc $\gamma$ RIIIa 158 V/V polymorphism, and endpoints approached significance with the Fc $\gamma$ RIIa H/H polymorphism [16]. In a separate study, the Fc $\gamma$ RIIa H/H genotype improved the pathological response rate in trastuzumab-based neoadjuvant chemotherapy and objective response rate in the metastatic setting [17]. The finding that Fc $\gamma$ RIIIa polymorphism H/H has efficacy against tumors suggests a role for monocytes in antibody-mediated tumor rejection. *In vivo* data from Fc $\gamma$ R knockout mice, clodronate depletion, and polymorphisms from human studies suggest a role of monocytes in antibody therapies that target cancer.

Although monocytes/macrophages have been shown to phagocytose antibody-opsonized tumor cells [15, 18, 19], the impact of antibody combinations, antigen density, Fc $\gamma$ R expression, and genotype have not been evaluated. To analyze these features, monocyte phagocytosis was compared to NK cells ADCC in a breast cancer model using tumor-targeting antibodies, trastuzumab and pertuzumab. In addition, Fc $\gamma$ R expression on monocyte and genotypes was analyzed to determine their impact on phagocytosis.

## Materials and methods

### Cell lines and cell culture

Breast cancer cell lines MCF-7 (3/27/12), T47D (12/8/11), HCC1500 (5/29/14), HCC1428 (5/29/14), HCC1419 (5/29/14), HCC1954 (5/29/14), BT474 (7/29/14), and SKBR3 (12/20/10) were obtained from ATCC (American Type Culture Collection, Manassas, VA). The dates of STR profiling showing authentication of the cell lines were last done for HCC 1954 (12/2/15), HCC 1419 and MCF-7 (9/24/15), and all other cell lines (9/15/15). MCF-7, T47D, and BT474 were cultured in DMEM supplemented with 10% FBS, 100 U/ml penicillin, and 100  $\mu$ g/ml streptomycin. HCC1419, HCC1428, HCC1500, and HCC1594 were cultured in RPMI 1640 medium supplemented with 10% FBS, 100 U/ml penicillin, and 100  $\mu$ g/ml streptomycin. SKBR3 was cultured in RPMI 1640 medium supplemented with 10% FBS, 1% pyruvate, 100 U/ml penicillin, and 100  $\mu$ g/ml streptomycin. Human peripheral blood mononuclear cells (PBMC) were purchased from HemaCare BioResearch Products (Van Nuys, CA). PBMC were thawed and cultured overnight in RPMI 1640 medium supplemented with 10% FBS, 100 U/ml penicillin, and 100  $\mu$ g/ml streptomycin in T75 TPP or Corning<sup>®</sup> ultra-low attachment surface tissue culture flasks.

### Gene modification of MCF-7 with human epidermal growth factor receptor 2 (HER2)

The MCF-7 cell line was modified with pcDNA3.1 (V79020), purchased from Thermo Fisher Scientific (Waltham, MA), or pcDNA3 HER2 WT, which was a gift from Mien-Chie Hung (Addgene plasmid # 16257) [20]. Vectors were transfected with Lipofectamine 3000 reagent using 2.5  $\mu$ g DNA-to-3.75  $\mu$ l Lipofectamine 3000 reagent, according to the manufacturer's instructions. Individual clones of MCF-7 HER2 were obtained by selection with 700  $\mu$ g/ml G418 and limiting dilution. HER2 expression was confirmed by flow cytometry.

### Antibodies

Anti-CD56 PE-Cy5 (Clone B159, 5/100  $\mu$ l, Cat. No. 555517), anti-CD3 Alexa Fluor (AF) 700 (Clone UCTH1, 3/100  $\mu$ l, Cat. No. 557943), anti-CD14 PE-CF594 (Clone M $\phi$ P9, 0.5/100  $\mu$ l, Cat. No. 562335), anti-CD16 Brilliant Violet 510 (Clone 3G8, 2/100  $\mu$ l, Cat. No. 563830), anti-CD16 FITC (Clone 3G8, 6.4/100  $\mu$ l, Cat. No. 555406), CD32 FITC (Clone FL18.26, 2  $\mu$ l/100, Cat. No. 555448), and anti-epithelial cell adhesion molecule (EpCAM) PE

(Clone EBA-1, 1.5/100  $\mu$ l) were purchased from BD Biosciences (San Jose, CA). Anti-CD107a eFluor660 (Clone eBioH4A3, 1/200  $\mu$ l, Cat. No. 50-1079-42), and anti-CD107b eFluor660 (Clone eBioH4B4, 1/200  $\mu$ l, Cat. No. 50-1078-42) were bought from eBioscience (San Diego, CA). Anti-HER2 Alexa Fluor 647 (Clone 24D2, 0.05/100  $\mu$ l, Cat. No. 324412) and anti-CD14 AF647 (Clone HCD14, 10  $\mu$ g/ml) was bought from BioLegend (San Diego, CA). Trastuzumab and pertuzumab were obtained from our institution's pharmacy.

### Phagocytosis, degranulation, and tumor cell death

To evaluate phagocytosis, degranulation, and tumor cell death, flow cytometry was performed as previously described with minor modifications [21]. In addition to anti-CD56, CD3, and CD14, EpCAM was added to the staining protocol. EpCAM was used to evaluate internalization of tumor cells by monocytes. Phagocytosis was determined by the number of double positive CD14<sup>+</sup>CFSE<sup>+</sup> cells divided by the total number of CD14<sup>+</sup> cells multiplied by 100. Background phagocytosis levels were subtracted to obtain the antibody-dependent phagocytosis. Calculations for degranulation and tumor cell death were previously described [21]. Enrichment of monocytes and NK cell was performed by negative selection using EasySep™ Human Monocyte Enrichment Kit without CD16 Depletion and EasySep Human NK cell Enrichment Kit, respectively, according to the manufacturer's instructions (Stemcell Technologies, Vancouver, Canada). The net mean and standard deviation of triplicate samples were plotted.

Quantum™ Simply Cellular® anti-Mouse for mouse monoclonal antibodies was used to quantify Fc $\gamma$ RIIa and Fc $\gamma$ RIIIa according to the manufacturer's instructions.

### Microscopy

Phagocytosis was performed as described above with a modification of using only anti-CD14 AF647 to detect monocytes. After antibody staining, 100  $\mu$ l was added to cytospin chambers in which slides were prepared using a Cytotech centrifuge. Cells were then dried, fixed with 4% paraformaldehyde, and stained with DAPI. Cells were washed twice with PBS, coverslips were added, and cells were evaluated for phagocytosis using an inverted microscope (1  $\times$  83, Olympus Corporation, Tokyo, Japan).

### Fc $\gamma$ RIIa and Fc $\gamma$ RIIIa blocking

Phagocytosis was performed as described with minor modifications. Trastuzumab was added at 200 ng/ml and Fc $\gamma$ R blocking reagents were added individually or combined at 10  $\mu$ g/ml each. The Fc $\gamma$ R blocking reagents, anti-Fc $\gamma$ RII

(Clone 7.3), and anti-Fc $\gamma$ RIIIa (Clone 3G8) were purchased from Ancell Corporation (Bayport, MN).

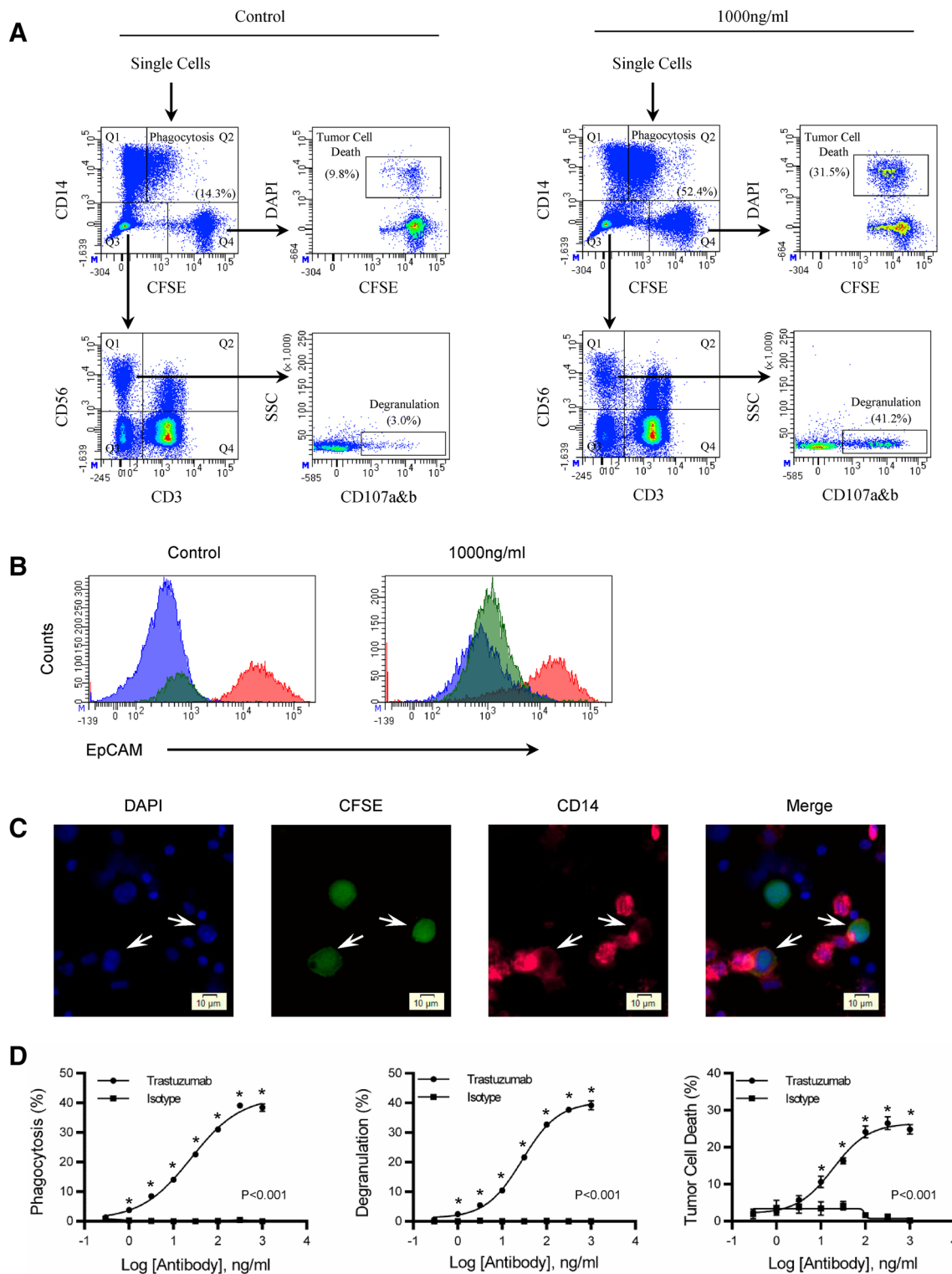
### Statistics/plots

Statistics and plots were generated using Prism 6 (GraphPad Software, La Jolla, CA). Plots were generated showing the mean  $\pm$  standard error of the mean and the regression line. To determine significance, two-way ANOVA with Sidak's multiple comparisons test, *T* tests, and one-way ANOVA with Tukey's multiple comparison's test were used.

## Results

### Simultaneous evaluation of monocyte phagocytosis, NK cell degranulation, and tumor cell death

To evaluate antibody-dependent phagocytosis, NK cell degranulation, and tumor cell death, PBMC were combined with CFSE-labeled HCC1419 and a half-log titration series of trastuzumab. After 4 h, cells were stained and evaluated for phagocytosis, NK cell degranulation, and tumor cell death by flow cytometry. Flow cytometry density plots of control and 1000 ng/ml are shown (Fig. 1a). Single cells were gated and phagocytosis was evaluated from the CD14 versus CFSE plot (Fig. 1a). Phagocytosis was determined by the number of CD14<sup>+</sup> cells that incorporated CFSE from tumor cells relative to the total number of CD14<sup>+</sup> cells. The quadrant gate that defined phagocytosis was determined by PBMC that were not co-cultured with CFSE-labeled tumor cells (Supplemental Fig. 1). The number in parenthesis shows the percentage of monocytes that have taken up tumor cells. To ensure that tumors were internalized, gates for CD14<sup>+</sup>/CFSE<sup>-</sup>, CD14<sup>+</sup>/CFSE<sup>+</sup>, and CD14<sup>-</sup>/CFSE<sup>+</sup> were generated and evaluated for EpCAM, a second-tumor antigen on HCC1419 (Fig. 1b). The CD14<sup>-</sup>/CFSE<sup>+</sup> tumor cell gate stains brightly with anti-EpCAM. In contrast, CD14<sup>+</sup>/CFSE<sup>-</sup> and CD14<sup>+</sup>/CFSE<sup>+</sup> gates stained dim with anti-EpCAM, suggesting that the CFSE-labeled tumor cells had been internalized by CD14<sup>+</sup> monocytes. NK cell degranulation was evaluated from the CD56<sup>+</sup>/CD3<sup>-</sup> population. This population is found among the double-negative (CD14<sup>-</sup>/CFSE<sup>-</sup>) population shown in the CD14 versus CFSE plot and evaluated for CD56 and CD3 expression (Fig. 1a). NK cell (CD56<sup>+</sup>CD3<sup>-</sup>) degranulation was determined by the percentage of NK cells that expressed CD107a&b relative to the total NK cell population. The number in parenthesis shows the percentage of NK cells that have degranulated. Tumor cell death was evaluated from CFSE-labeled tumor cells. In the CD14 versus CFSE plot, CFSE-gated tumor cells were evaluated for DAPI. Tumor



cell death is the percentage of tumor cells labeled DAPI<sup>+</sup>/CFSE<sup>+</sup> relative to the total number of tumor cells. The number in parenthesis shows the percentage of tumor cell death.

To ensure that CFSE-labeled tumors were not just binding monocytes, we compared them with NK cells labeled

with CFSE (Supplemental Fig. 2). CFSE was found to be associated with 52% of monocyte compared to 2% of NK cells, suggesting that monocytes were actively targeting tumor cells. To confirm that monocytes could independently perform phagocytosis, enriched monocytes (Supplemental

**Fig. 1** Simultaneous evaluation of antibody-dependent phagocytosis, NK cell degranulation, and tumor cell death. A 10:1 PBMC-to-tumor ratio was used to evaluate antibody-mediated effector function over a 4 h period. **a** See the “Results” section of this manuscript for a description of the gating strategy. Flow cytometry dot plots show control and 1000 ng/ml of trastuzumab. Values of phagocytosis, degranulation, and tumor cell death are in parenthesis. **b** To confirm phagocytosis, a second-tumor antigen EpCAM was used to determine if the monocytes internalized the tumor or not. Tumor cells (Q4) and monocyte (Q1 and Q2) were gated from the CD14 versus CFSE plot. Tumor cells are the red histogram, monocytes that have phagocytized tumors are the green histogram, and monocytes without tumor cells are the blue histograms. **c** Microscopy showing monocyte phagocytosis of tumor cells. Nuclei are stained with DAPI (Blue), HCC1419 (Green), and CD14 monocytes (Pink). Trastuzumab was used at 100 ng/ml and the images are from a trastuzumab co-culture of PBMC and HCC1419. **d** Titration curves of degranulation, tumor cell death, and phagocytosis comparing trastuzumab with isotype control. Background levels of phagocytosis, degranulation, and tumor cell death are subtracted from experimental values. All samples were performed in triplicate; means  $\pm$  SEM and regression line are plotted on the graph. Two-way ANOVA with Sidak’s multiple comparisons test was used to determine significance. The asterisk represents significance between trastuzumab and isotype control. Results are representative of three independent experiments

Fig. 3) were found to phagocytose tumor cells consistent with what was observed with PBMC (Supplemental Fig. 4). However, when purified NK cells were added back into the enriched monocyte population, there was an increase in phagocytosis (Supplemental Fig. 4c). To verify that NK cells were associated with degranulation and tumor cell death, isolated NK cells were co-cultured with HCC1419 and trastuzumab and evaluated for phagocytosis, degranulation, and tumor cell death. NK cell degranulation (Supplemental Fig. 5) and tumor cell death (Supplemental Fig. 6) were found with co-cultures enriched with NK cells. In contrast, there was significantly less cell death associated with enriched monocytes (Supplemental Fig. 5). Interestingly, when the enriched monocyte population was evaluated for NK cell degranulation, residual NK cells had insignificant degranulation between control and trastuzumab treatments (Supplemental Fig. 7). However, tumor cell death was significant within the co-culture which may suggest that monocytes modestly contribute to cellular cytotoxicity within the 4 h assay (Supplemental Fig. 7).

Fluorescent microscopy was used to confirm phagocytosis. Arrows indicate tumors undergoing phagocytosis (Fig. 1c). Analysis of the CD14 stain shows membranes extending from an adjacent monocyte to surround individual tumor cells (Fig. 1c). Monocyte phagocytosis on the left is more complete than on the right, as the membrane almost completely surrounds the tumor cell compared to 50% of the tumor cell observed on the right. In the merged image, the CD14 stain overlaps the CFSE-labeled tumors which suggests phagocytosis involved the engulfment of whole tumor cells (Fig. 1c). A third tumor cell is

also observed in the image and appears to be surrounded by lymphocytes, perhaps NK cells. There is no CD14 staining associated with this tumor cell, indicating the staining is specific for monocytes and that monocytes need to be in the proximity of tumors for phagocytosis. Quantitatively, trastuzumab (48.9%) was significantly ( $P < 0.02$ ) greater than isotype control (21.0%) when evaluating phagocytosis by microscopy.

To show that antibody-opsonized tumors are required for effector function, trastuzumab was compared to isotype controls in the assay. As the antibody concentration increased, from 0.3 to 1000 ng/ml, there is an increase in phagocytosis, NK cell degranulation, and tumor cell death in trastuzumab treated co-cultures and not in isotype controls. The increase in trastuzumab concentration shows that phagocytosis, NK cell degranulation, and tumor cell death are trastuzumab-dependent and can be simultaneously evaluated from the same sample (Fig. 1d).

### Increased avidity enhances monocyte phagocytosis but not NK cell-mediated ADCC

To determine if an increase in avidity may enhance phagocytosis, a second HER2 antibody, pertuzumab, was combined with trastuzumab and compared to the individual antibodies and isotype control. Consistent with the observation of Scheuer et al., the combination of pertuzumab and trastuzumab showed no difference in tumor cell death when compared to pertuzumab or trastuzumab (Fig. 2a). In contrast, there was an increase in phagocytosis when the combination of antibodies was compared to the individual antibodies alone when targeting the HER2 gene-amplified cell line HCC1419 (Fig. 2b). The combination of pertuzumab and trastuzumab has a two-to-threefold increase in potency over the individual antibodies alone. Similar phagocytosis results were observed when pertuzumab and trastuzumab were used to target the HER2 gene-amplified cell lines BT-474 and SKBR3. In contrast, HER2 non-gene-amplified tumors failed to increase phagocytosis when the combination of pertuzumab and trastuzumab was compared to the individual antibodies (Supplemental Fig. 8). However, when low HER2 levels were evaluated for degranulation and tumor cell death, avidity may have influenced NK cell activity (Supplemental Fig. 9).

To determine if an increase in avidity could explain the enhancement in phagocytosis, pertuzumab and trastuzumab were used to stain HCC1419 breast tumor cells. The combination of antibodies enhanced the mean fluorescence intensity, indicating an increase in antibody binding to HER2 (Fig. 2c). Enhanced antibody binding to HER2 may facilitate increased Fc $\gamma$ R interactions that heighten the avidity. To determine if Fc $\gamma$ R are more available on monocytes than on NK cells, quantitative flow cytometry was used to evaluate

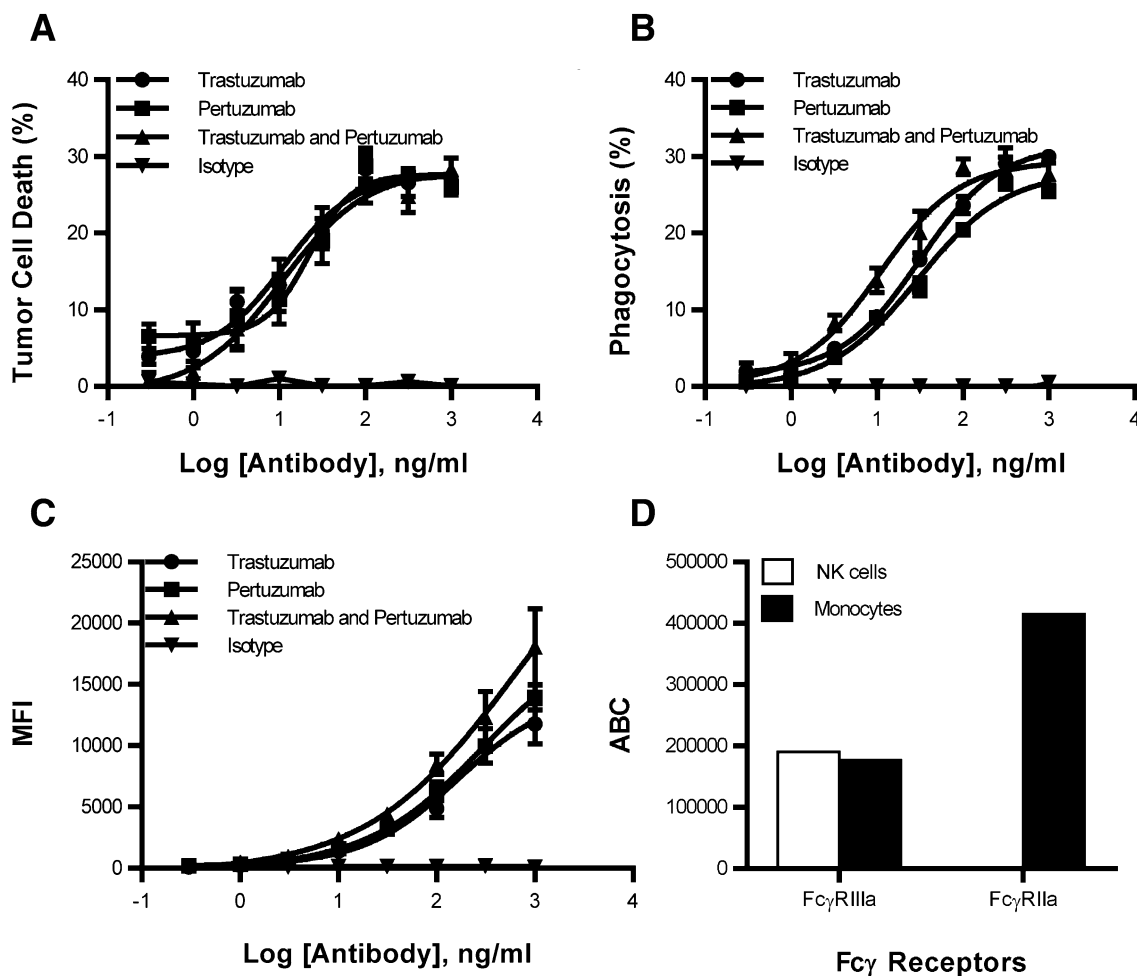


**Fig. 2** Combination of trastuzumab and pertuzumab enhanced monocyte phagocytosis by increasing avidity. A half-log titration series evaluating trastuzumab, pertuzumab, trastuzumab + pertuzumab, and isotype control were used to evaluate (a) tumor cell death and (b) phagocytosis. c Staining of HCC1419 with pertuzumab and trastuzumab which was detected with a secondary goat anti-human PE

antibody. All samples were performed in triplicate; means  $\pm$  SEM and regression line are plotted on the graph. Two-way ANOVA with Sidak's multiple comparisons test was used to determine significance. Asterisk represents significance between trastuzumab and pertuzumab compared to trastuzumab or pertuzumab. d Quantitative flow cytometry was used to measure Fc $\gamma$ RII and Fc $\gamma$ RIIIa expression

Fc $\gamma$ RII and Fc $\gamma$ RIIIa. Fc $\gamma$ RIIIa expression was similar on the two cell types, while Fc $\gamma$ RII was expressed uniquely on monocytes (Fig. 2d). The overall number of Fc $\gamma$ R was higher on monocytes, providing a means to increase the avidity of antibody Fc bound to tumor cells. The data show that increasing avidity with the addition of a second antibody leads to enhanced monocyte phagocytosis.

### Monocyte phagocytosis requires higher antigen density than NK cell-mediated ADCC

To compare the activation requirements between monocytes and NK cells, titrations of trastuzumab were added to PBMC and CFSE-labeled tumor cells to evaluate phagocytosis, NK cell degranulation, and tumor cell death. Trastuzumab-targeted SKBR3, an HER2 gene-amplified

cell line, had an increase in monocyte phagocytosis and NK cell degranulation compared to T47D, a HER2 non-gene-amplified cell line (Fig. 3a). However, tumor cell death between the two cell lines was the same (Fig. 3a). To determine if other cell lines were consistent with these results, several HER2 gene-amplified (SKBR3, HCC1419, BT474, and HCC1954) and non-amplified (T47D, MCF-7, HCC1428, and HCC1500) breast cancer cell lines were evaluated for phagocytosis, NK cell degranulation, and tumor cell death at a trastuzumab concentration of 316 ng/ml (Fig. 3b). In most samples, that concentration maximized the efficacy of phagocytosis, NK cell degranulation, and tumor cell death in HER2 gene-amplified and non-amplified tumor cell lines. Each cell line was tested a minimum of two times. In HER2 non-amplified tumor cells, the

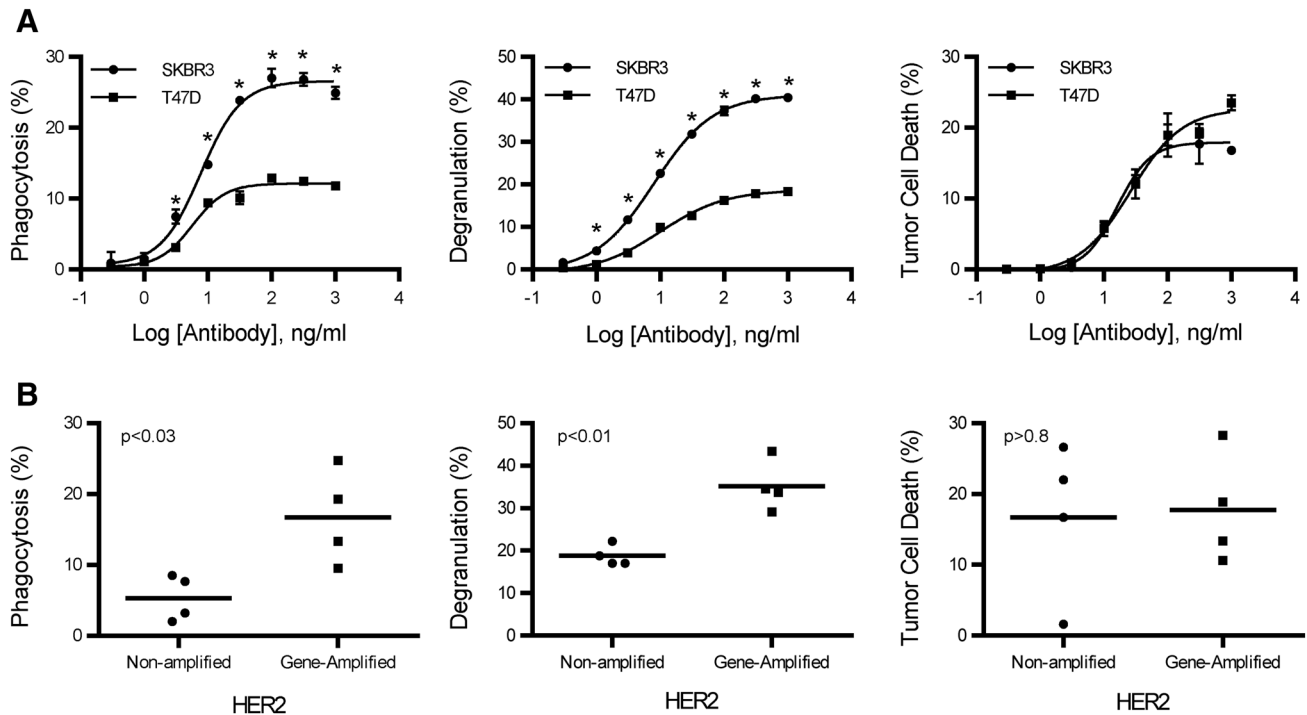


**Fig. 3** Monocyte phagocytosis is increased with HER2 gene-amplified targets. Antibody-dependent phagocytosis, degranulation, and tumor cell death were evaluated on HER2-amplified and -non-amplified tumor cell lines. **a** Titration curves of antibody-dependent phagocytosis, degranulation, and tumor cell death from SKBR3 (HER2 amplified) and T47D (HER2 non-amplified) tumor cell lines. All samples were performed in triplicate; means  $\pm$  SEM and regression line are plotted on the graph. Two-way ANOVA with Sidak's multiple comparisons test was used to determine significance. Asterisk

represents significance between SKBR3 and T47D. **b** Comparison between antibody-dependent phagocytosis, degranulation, and tumor cell death of breast cancer cell lines that are amplified and non-amplified for HER2. Each point on the graph represents a different cell line and is the mean of a minimum of two experiments at the trastuzumab concentration of 316 ng/ml. Two tailed *t* tests were used to obtain *P* values for phagocytosis ( $P < 0.03$ ), NK cell degranulation ( $P < 0.01$ ), and tumor cell death ( $P > 0.8$ )

mean phagocytosis of the four cell lines was  $5.3 \pm 1.6\%$ , whereas the mean of the gene-amplified cell lines was  $16.7 \pm 3.3\%$ . There is approximately a threefold increase in phagocytosis in HER2 gene-amplified compared to non-amplified cell lines. NK cell degranulation in non-amplified and gene-amplified tumor cells was found to be  $18.8 \pm 1.2$  and  $35.1 \pm 3.0\%$ , respectively. Monocyte phagocytosis ( $P < 0.03$ ) and NK cell degranulation ( $P < 0.01$ ) were significantly greater in HER2 gene-amplified tumor cells. However, there was no difference ( $P > 0.8$ ) in tumor cell death between HER2 non-amplified cells and gene-amplified cells at  $16.7 \pm 5.4$  and  $17.8 \pm 3.9\%$ , respectively. These data indicate that monocyte phagocytosis and NK cell degranulation improve as the antigen density increases on tumor cells. However, the percentage of tumor cell death mediated by NK cells between HER2 non-amplified and gene-amplified tumor cells is the same, a finding that suggests NK cell degranulation does not correlate with tumor cell death. The data also suggest that monocyte

phagocytosis requires higher antigen density than NK cells for activation.

### Phagocytosis is antigen density-dependent

It is possible that regulatory elements on cells may influence phagocytosis; therefore, to determine whether higher antigen density contributes to increased phagocytosis MCF-7 was modified to overexpress HER2 as a means to eliminate regulatory factors that may be expressed on various cell lines. An approximate tenfold increase in HER2 protein expression was obtained in HER2-transfected MCF-7 compared to vector control cells (Fig. 4a). When evaluated for phagocytosis activity, MCF-7 cells with increased HER2 expression were significantly ( $P < 0.001$ ) more susceptible to monocyte phagocytosis (Fig. 4b). Overexpression of HER2 in MCF-7 enhanced NK cell degranulation ( $P < 0.001$ ), but there were marginal changes if any in tumor cell death ( $P > 0.3$ ) (Supplemental Fig. 10). The overexpressed HER2 on MCF-7 and gene-amplified breast cancer cells confirm that higher

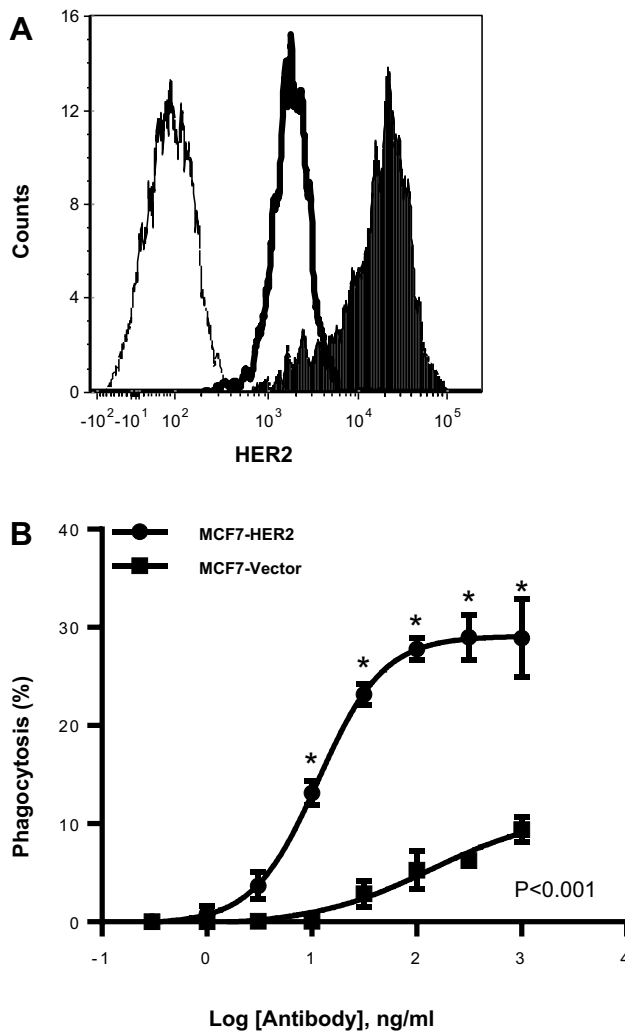


**Fig. 4** Antigen density is important for phagocytosis. The MCF-7 breast cancer cell line was transfected with pcDNA HER2, and individual clones were selected by serial dilution. **a** Characterization of the protein expression by flow cytometry. Filled histogram is pcDNA HER2, bold line is empty vector, and normal line is unstained control. **b** Phagocytosis was performed as previously described in Fig. 1. Phagocytosis was performed in triplicate; means  $\pm$  SEM and regression line are plotted on the graph. Two-way ANOVA with Sidak's multiple comparisons test was used to determine significance. Asterisk represents significance between MCF7-HER2 and MCF7-Vector

antigen density improves monocyte antibody-dependent phagocytosis.

### Monocyte activation and Fc $\gamma$ R are important in phagocytosis

Monocytes have multiple types of Fc $\gamma$ R on the cell surface that is involved in antibody-dependent phagocytosis. To determine if there is a preferential use of Fc $\gamma$ RIIa or Fc $\gamma$ RIIIa in phagocytosis, the addition of anti-Fc $\gamma$ RIIIa was added to the staining procedure to separate Fc $\gamma$ RIIIa<sup>+</sup> from Fc $\gamma$ RIIIa<sup>-</sup> monocytes.

However, the Fc $\gamma$ RIIIa staining failed to define clear differences between Fc $\gamma$ RIIIa<sup>+</sup> and Fc $\gamma$ RIIIa<sup>-</sup> monocytes when evaluating phagocytosis (data not shown). It was observed that Fc $\gamma$ RIIIa<sup>+</sup> was expressed on 5–10% of freshly thawed monocytes. After being cultured overnight in tissue culture-treated flasks >65% of monocytes expressed Fc $\gamma$ RIIIa (Fig. 5a). In contrast, when a non-adherent plate was used Fc $\gamma$ RIIIa<sup>+</sup> was not upregulated on monocytes (Fig. 5a). When monocytes from adherent and non-adherent plates were compared for phagocytosis, the monocytes from the adherent flask had enhanced phagocytic activity compared to the non-adherent flask (Fig. 5b). This showed that Fc $\gamma$ RIIIa enhanced the antibody-dependent response beyond that of Fc $\gamma$ RIIa. Given that the monocytes in the assay upregulated Fc $\gamma$ RIIIa, blocking Fab fragments were employed to determine if there was a preference for Fc $\gamma$ RIIa or Fc $\gamma$ RIIIa in mediating phagocytosis. Fc $\gamma$ RIIa and Fc $\gamma$ RIIIa were blocked by Fab molecules, showing that monocytes use both receptor types in phagocytosis (Fig. 5c). Blockade of Fc $\gamma$ RIIIa inhibited phagocytosis to a greater extent than Fc $\gamma$ RIIa, suggesting that Fc $\gamma$ RIIIa may have a slightly greater role in the process. These data lend credence to a hypothesis that monocytes may require an activation event to enhance antibody-dependent phagocytosis and that the increase in activity is associated with an increase in Fc $\gamma$ RIIIa.

### Influence of genotype on Fc $\gamma$ RIIIa and Fc $\gamma$ RIIa

The valine (V) at position 158 of Fc $\gamma$ RIIIa has a higher affinity for IgG1 than phenylalanine (F), while the histidine (H) at position 131 of Fc $\gamma$ RIIa has a slightly higher affinity for IgG1 than the arginine (R) [19]. To determine if the polymorphism of Fc $\gamma$ RIIIa at position 158 and Fc $\gamma$ RIIa at position 131 influences phagocytosis, multiple PBMC were genotyped and evaluated for phagocytosis. The distribution of Fc $\gamma$ RIIIa at position 158 was VV=0.10, VF=0.35, and FF=0.55, and distribution of Fc $\gamma$ RIIa at position 131 was HH=0.32, HR=0.39, and RR=0.29. Phagocytosis was significantly greater with Fc $\gamma$ RIIIa VV and VF ( $P < 0.01$ ) when compared to the FF phenotype (Fig. 6a). No difference in phagocytosis was observed in Fc $\gamma$ RIIa HH ( $P > 0.10$ ), HR, or RR genotypes (Fig. 6b). Having at least one V at position 158 in Fc $\gamma$ RIIIa enhanced phagocytosis, and the homozygous HH at position 131 of Fc $\gamma$ RIIa trended toward increased phagocytic activity. Fc $\gamma$ RIIIa VV and VF genotypes were found to enhance tumor cell death, whereas Fc $\gamma$ RIIa genotype had no effect (Supplemental Fig. 11).

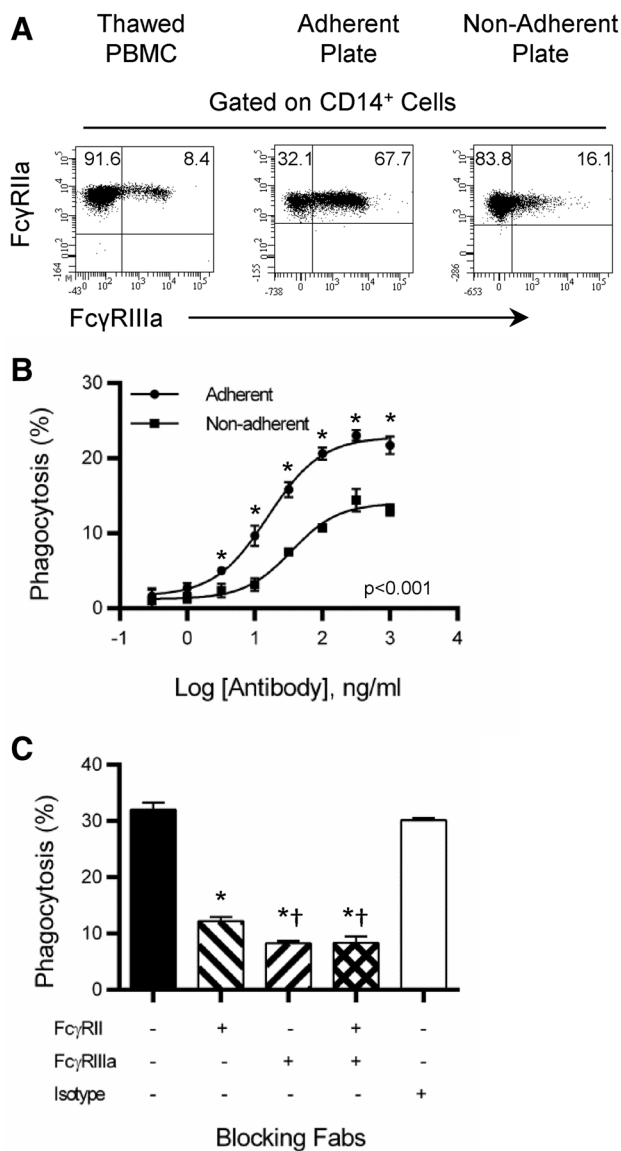


**Fig. 5** FcγRIIa and FcγRIIIa involved with phagocytosis of tumors. **a** Expression of FcγRIIa and FcγRIIIa from thawed PBMC and those cultured overnight on adherent and non-adherent tissue culture flasks. **b** Phagocytosis was evaluated as described in Fig. 1. Comparison of phagocytosis from PBMC cultured in adherent and non-adherent tissue culture flasks. All samples were performed in triplicate; means ± SEM and regression line are plotted on the graph. Two-way ANOVA with Sidak’s multiple comparisons test was used to determine the significance. Asterisk represents significance between adherent and non-adherent. Results are representative of two independent experiments. **c** Phagocytosis was evaluated as described in Fig. 1 with a single concentration of trastuzumab (200 ng/ml). FcγRIIa and FcγRIIIa Fab were used at a concentration of 10 μg/ml. All samples were performed in triplicate; means ± SEM are plotted on the graph. One-way ANOVA with Tukey’s multiple comparisons test was used to determine significance. Asterisk represents significance between untreated and isotype controls and blocking antibodies. †Represents significance between blocking of FcγRIIa and FcγRIIIa or FcγRIIa + FcγRIIIa. Results are representative of two independent experiments

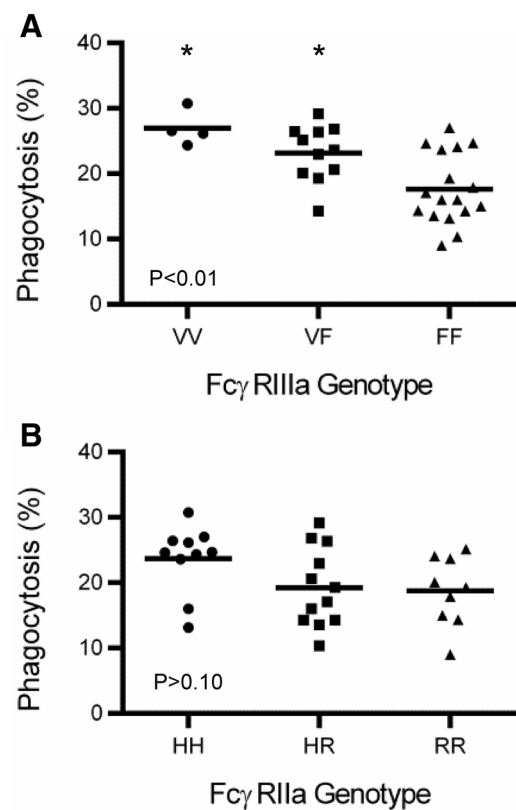


**Fig. 6** FcγRIIIa 158V enhances monocyte phagocytosis. PBMC from multiple donors were evaluated for phagocytosis as described in Fig. 1. Genotypes were obtained for FcγRIIIa at position 158 (V/F) and FcγRIIa position 131(H/R). PBMC were then separated into groups based on genotype for FcγRIIIa (**a**) and FcγRIIa (**b**). Each symbol is representative of one individual’s PBMC. One-way ANOVA with Tukey’s multiple comparisons test was used to determine significance. Asterisk represents significance between VV or VF and FF

**Discussion**

Monocytes/macrophages have been shown to be important mediators of antibody-mediated effector functions in vivo [13–15]. The depletion of monocytes in animals when treating tumors with antibodies eliminated the therapeutic efficacy of the antibody [14, 15]. Not surprisingly, we found that monocytes respond differently than NK cells to opsonized tumor cells. While monocytes increased their potency with a combination of trastuzumab and pertuzumab compared to the individual antibodies, NK cell-mediated ADCC was not influenced by a second antibody targeting an alternative epitope on the same protein. Second, the increase in antigen density significantly enhanced monocyte and NK cell function, but failed to increase tumor cell death in HER2 gene-amplified cell lines. Phagocytosis was enhanced by an activation event that increased expression of FcγRIIIa. If the increase in FcγRIIIa was the high-affinity (V158) polymorphism, the receptor could enhance phagocytosis compared

to the low-affinity polymorphism. These findings indicate that monocyte function is enhanced by Fc $\gamma$ R expression, and the genotype, antigen density, and avidity associated with multiple antibodies binding to the tumor target.

In preclinical and clinical treatments of breast cancer, the combination of pertuzumab and trastuzumab has improved tumor rejection and overall survival [1, 9]. This may be due to the blockade of signal transduction and prevention of cellular growth [22, 23] or potentially to monocyte effector function. We observed enhanced monocyte phagocytosis potency when cells were treated with the combination of pertuzumab and trastuzumab as compared to the individual antibodies alone. The recent report that trastuzumab requires the monocyte/macrophage network to reject tumors in mice [15] supports monocyte function and potentially phagocytosis as a mechanism of tumor rejection. Given that pertuzumab and trastuzumab bind to different epitopes on HER2 [24, 25], a working hypothesis could be that the combination of antibodies enhances the avidity of tumors by increasing the number of Fc regions available for recognition by enhanced numbers of Fc $\gamma$ Rs found on monocytes.

In contrast, the addition of pertuzumab to trastuzumab had no effect on NK cell-mediated killing of tumors, consistent with the findings of Scheuer et al. [9]. Although we saw an increase in NK cell degranulation associated with HER2 density, the degree of tumor cell death was insignificant between gene-amplified and non-amplified breast tumor cells. In multiple studies, NK cells at fixed effector-to-target ratios have shown breast cancer cell death is independent of antigen density [26–28]. This is in contrast to other studies that show that NK cell-mediated ADCC is associated with increased antigen density [4, 5]. Collins et al. noted if the effector-to-target ratio was increased, ADCC of high-density tumor cells is also increased, suggesting that the number of NK cells could be limiting [26]. However, tamoxifen-induced HER2 levels increased NK cell degranulation and tumor cell death in HER2 non-amplified cell lines [21], indicating that similar ratios of NK cells respond to greater antigen density. One explanation is NK cells have a threshold of activation when engaging antibody-opsonized tumors. Tumors that have low antigen density may start to initiate NK cell degranulation and tumor cell death. As the density of the target receptor increases, a threshold for Fc $\gamma$ R signaling is reached, inducing tumor cell death. Additional signaling may not be required to enhance tumor cell death. Support for this was observed when pertuzumab and trastuzumab were found to enhance NK cell activity on tumor cells with low HER2 expression. As antigen density increases the differential effect of combining antibodies also disappears until monocyte function requires it. Alternatively, intrinsic factor(s) in tumor cells may limit the effects of NK cell-mediated ADCC. X-linked inhibitor of apoptosis protein (XIAP), a caspase binding protein has been shown to

decrease ADCC [29]. Intrinsic regulators such as XIAP may provide tumors a method to mitigate the cytotoxic effector function of immune cells.

Antigen density has proven to be of great importance for the treatment of patients with HER2 gene-amplified tumors with trastuzumab. Trastuzumab increased time to progression and overall survival among patients that had HER2 gene-amplification as determined by fluorescence in situ hybridization (FISH), while for patients' tumors that were FISH-negative trastuzumab had no effect, and the treatment was comparable to chemotherapy alone [30]. In our experience, monocyte phagocytosis was significantly more efficient at higher antigen density. The increased requirement of antigen density for monocytes that we observed may be attributed to Fc $\gamma$ RIIb expression. NK cells do not express the receptor [13] and appear to be more easily activated by low levels of antigen expression on tumor cells than monocytes. Clynes et al. demonstrated that mice deficient of the inhibitory receptor Fc $\gamma$ RIIb have a greater capacity to reject tumors when treated with antibodies [13]. However, when blocking antibodies were used to inhibit Fc $\gamma$ RIIb engagement in vitro, there was no difference in the level of human macrophage phagocytosis in controls versus those blocked with Fc $\gamma$ RIIb [19]. This may suggest that the mouse inhibitory Fc $\gamma$ R is functionally different than human inhibitory Fc $\gamma$ R. In contrast, the depletion of activating Fc $\gamma$ Rs in mouse models [13] and in vitro blocking of Fc $\gamma$ RII(a) and/or Fc $\gamma$ RIIIa by our own and other studies [15, 19] show the importance of the low-affinity activating receptors in tumor rejection and phagocytosis, respectively.

Only a small percentage of monocytes in the blood express Fc $\gamma$ RIIIa and all express Fc $\gamma$ RIIa. We observed that overnight culture resulted in increased expression of Fc $\gamma$ RIIIa that resulted in improved phagocytosis. The tumor microenvironment modifies monocyte/macrophage function. On one extreme, inflammatory macrophages (M1) promote tumor rejection; on the other, macrophages (M2) assist in tumor growth, invasion, and metastasis [31]. The ability to modify monocyte function to increase tumor rejection will be of great importance. It is well known that interferon- $\gamma$  (IFN- $\gamma$ ) is a potent activator of M1 macrophages that improves the cells' oxidative burst and phagocytosis [15]. Treatment of THP-1 cells with IFN- $\gamma$  elevated Fc $\gamma$ RIIIa that resulted in improved phagocytosis [15]. Interestingly, heightened expression of Fc $\gamma$ RIIIa comes with enhanced affinity for IgG1 [19] which is strengthened further with the V158 genotype. It is possible that IFN- $\gamma$  is critical for monocyte activation in controlling tumor growth and development. In syngeneic mouse models of ErbB-2 antibody therapy, perforin and tumor necrosis factor- $\alpha$  were found to be dispensable, but type 1 interferons and IFN- $\gamma$  were important in tumor rejection [12]. By contrast, M2 macrophages have been observed to enhance and inhibit phagocytosis in

breast cancer and leukemic targets, respectively [31, 32]. Additional studies will be required to better understand how the tumor microenvironment influences macrophage polarization and function.

Monocytes/macrophages are among the highest number of leukocytes found in human tumors [33]. Therapeutic antibodies can trigger monocyte effector functions such as phagocytosis [15, 18], trogocytosis [34], and release of cytotoxic oxygen and nitrogen free-radicals [35]. These effector mechanisms may lead to tumor destruction and/or T-cell activation that can potentiate the immune response against the tumor [36]. Indeed, in patients treated with trastuzumab, remissions were found to be associated with an increase in lymphocytes and leukocytes [37]. In breast cancer, less than 50% of macrophages express FcγRIIIa [33], which we found to enhance phagocytosis. A better understanding on how to facilitate the expression of FcγRIIIa and activation of monocytes/macrophage effector mechanisms may provide improved methods to treat cancer.

**Acknowledgements** We would like to acknowledge Sandra Kear for editing.

**Author contributions** JY: performed experiments and analyzed the data. AJA: performed experiments and analyzed the data. TSS: performed experiments and analyzed the data. GTR: performed experiments and analyzed the data. JOR: conceived and designed experiments, performed experiments, analyzed the data, contributed reagents/materials/analysis tools, and wrote the paper.

**Funding** This research was supported by an Aurora Cancer Care Research Award (505-3979) funded by the Vince Lombardi Cancer Foundation with the Aurora Research Institute and with Aurora Research Institute Institutional Funds.

## Compliance with ethical standards

**Conflict of interest** The authors declare no conflict of interest.

**Ethical approval and ethical standards** PBMC were purified from apheresis products obtained from consented individuals under protocol BC 10-07 (Blood Center of Wisconsin, Milwaukee, WI).

## References

- Seidel UJ, Schlegel P, Lang P (2013) Natural killer cell mediated antibody-dependent cellular cytotoxicity in tumor immunotherapy with therapeutic antibodies. *Front Immunol* 4:76. <https://doi.org/10.3389/fimmu.2013.00076>
- Koene HR, Kleijer M, Algra J, Roos D, von dem Borne AE, de HM (1997) Fc gammaRIIIa-158V/F polymorphism influences the binding of IgG by natural killer cell Fc gammaRIIIa, independently of the Fc gammaRIIIa-48L/R/H phenotype. *Blood* 90:1109–1114
- Liu Q, Sun Y, Rihn S, Nolting A, Tsoukas PN, Jost S, Cohen K, Walker B, Alter G (2009) Matrix metalloprotease inhibitors restore impaired NK cell-mediated antibody-dependent cellular cytotoxicity in human immunodeficiency virus type 1 infection. *J Virol* 83:8705–8712. <https://doi.org/10.1128/JVI.02666-08>
- Tang Y, Lou J, Alpaugh RK, Robinson MK, Marks JD, Weiner LM (2007) Regulation of antibody-dependent cellular cytotoxicity by IgG intrinsic and apparent affinity for target antigen. *J Immunol* 179:2815–2823
- Velders MP, van Rhijn CM, Oskam E, Fleuren GJ, Warnaar SO, Litvinov SV (1998) The impact of antigen density and antibody affinity on antibody-dependent cellular cytotoxicity: relevance for immunotherapy of carcinomas. *Br J Cancer* 78: 478–83
- Wu J, Edberg JC, Redecha PB, Bansal V, Guyre PM, Coleman K, Salmon JE, Kimberly RP (1997) A novel polymorphism of FcγRIIIa (CD16) alters receptor function and predisposes to autoimmune disease. *J Clin Invest* 100:1059–1070. <https://doi.org/10.1172/JCI119616>
- Mohsin SK, Weiss HL, Gutierrez MC et al (2005) Neoadjuvant trastuzumab induces apoptosis in primary breast cancers. *J Clin Oncol* 23:2460–2468. <https://doi.org/10.1200/JCO.2005.00.661>
- Tagliabue E, Campiglio M, Pupa SM, Menard S, Balsari A (2012) Activity and resistance of trastuzumab according to different clinical settings. *Cancer Treat Rev* 38:212–217. <https://doi.org/10.1016/j.ctrv.2011.06.002>
- Scheuer W, Friess T, Burtscher H, Bossenmaier B, Endl J, Hasmann M (2009) Strongly enhanced antitumor activity of trastuzumab and pertuzumab combination treatment on HER2-positive human xenograft tumor models. *Cancer Res* 69:9330–9336. <https://doi.org/10.1158/0008-5472.CAN-08-4597>
- Swain SM, Baselga J, Kim SB et al (2015) Pertuzumab, trastuzumab, and docetaxel in HER2-positive metastatic breast cancer. *N Engl J Med* 372:724–34. <https://doi.org/10.1056/NEJMoa1413513>
- Swain SM, Kim SB, Cortes J et al (2013) Pertuzumab, trastuzumab, and docetaxel for HER2-positive metastatic breast cancer (CLEOPATRA study): overall survival results from a randomised, double-blind, placebo-controlled, phase 3 study. *Lancet Oncol* 14:461–71. [https://doi.org/10.1016/S1470-2045\(13\)70130-X](https://doi.org/10.1016/S1470-2045(13)70130-X)
- Stagg J, Loi S, Divisekera U, Ngoi SF, Duret H, Yagita H, Teng MW, Smyth MJ (2011) Anti-ErbB-2 mAb therapy requires type I and II interferons and synergizes with anti-PD-1 or anti-CD137 mAb therapy. *Proc Natl Acad Sci USA* 108:7142–7. <https://doi.org/10.1073/pnas.1016569108>
- Clynes RA, Towers TL, Presta LG, Ravetch JV (2000) Inhibitory Fc receptors modulate in vivo cytotoxicity against tumor targets. *Nat Med* 6:443–446. <https://doi.org/10.1038/74704>
- Uchida J, Hamaguchi Y, Oliver JA, Ravetch JV, Poe JC, Haas KM, Tedder TF (2004) The innate mononuclear phagocyte network depletes B lymphocytes through Fc receptor-dependent mechanisms during anti-CD20 antibody immunotherapy. *J Exp Med* 199:1659–1669. <https://doi.org/10.1084/jem.20040119>
- Shi Y, Fan X, Deng H et al (2015) Trastuzumab triggers phagocytic killing of high HER2 cancer cells in vitro and in vivo by interaction with Fcγ receptors on macrophages. *J Immunol* 194:4379–4386. <https://doi.org/10.4049/jimmunol.1402891>
- Musolino A, Naldi N, Bortesi B et al (2008) Immunoglobulin G fragment C receptor polymorphisms and clinical efficacy of trastuzumab-based therapy in patients with HER-2/neu-positive metastatic breast cancer. *J Clin Oncol* 26:1789–1796. <https://doi.org/10.1200/JCO.2007.14.8957>
- Tamura K, Shimizu C, Hojo T et al (2011) FcγRIIb and 3A polymorphisms predict clinical outcome of trastuzumab in both neoadjuvant and metastatic settings in patients with HER2-positive breast cancer. *Ann Oncol* 22:1302–1307. <https://doi.org/10.1093/annonc/mdq585>
- Lazar GA, Dang W, Karki S et al (2006) Engineered antibody Fc variants with enhanced effector function. *Proc Natl Acad Sci USA* 103:4005–10. <https://doi.org/10.1073/pnas.0508123103>

19. Richards JO, Karki S, Lazar GA, Chen H, Dang W, Desjarlais JR (2008) Optimization of antibody binding to FcγRIIIa enhances macrophage phagocytosis of tumor cells. *Mol Cancer Ther* 7:2517–2527. <https://doi.org/10.1158/1535-7163.MCT-08-0201>
20. Li YM, Pan Y, Wei Y et al (2004) Upregulation of CXCR4 is essential for HER2-mediated tumor metastasis. *Cancer Cell* 6: 459–69. <https://doi.org/10.1016/j.ccr.2004.09.027>
21. Richards JO, Albers AJ, Smith TS, Tjoe JA (2016) NK cell-mediated antibody-dependent cellular cytotoxicity is enhanced by tamoxifen in HER2/neu non-amplified, but not HER2/neu-amplified, breast cancer cells. *Cancer Immunol Immunother* 65:1325–1335. <https://doi.org/10.1007/s00262-016-1885-7>
22. Adams CW, Allison DE, Flagella K, Presta L, Clarke J, Dybdal N, McKeever K, Sliwkowski MX (2006) Humanization of a recombinant monoclonal antibody to produce a therapeutic HER dimerization inhibitor, pertuzumab. *Cancer Immunol Immunother* 55:717–27. <https://doi.org/10.1007/s00262-005-0058-x>
23. Franklin MC, Carey KD, Vajdos FF, Leahy DJ, de Vos AM, Sliwkowski MX (2004) Insights into ErbB signaling from the structure of the ErbB2-pertuzumab complex. *Cancer Cell* 5: 317–28
24. Cho HS, Mason K, Ramyar KX, Stanley AM, Gabelli SB, Denny DW Jr, Leahy DJ (2003) Structure of the extracellular region of HER2 alone and in complex with the Herceptin Fab. *Nature* 421:756–60. <https://doi.org/10.1038/nature01392>
25. Fendly BM, Winget M, Hudziak RM, Lipari MT, Napier MA, Ullrich A (1990) Characterization of murine monoclonal antibodies reactive to either the human epidermal growth factor receptor or HER2/neu gene product. *Cancer Res* 50:1550–1558
26. Collins DM, O'Donovan N, McGowan PM, O'Sullivan F, Duffy MJ, Crown J (2012) Trastuzumab induces antibody-dependent cell-mediated cytotoxicity (ADCC) in HER-2-non-amplified breast cancer cell lines. *Ann Oncol* 23:1788–1795. <https://doi.org/10.1093/annonc/mdr484>
27. Cooley S, Burns LJ, Repka T, Miller JS (1999) Natural killer cell cytotoxicity of breast cancer targets is enhanced by two distinct mechanisms of antibody-dependent cellular cytotoxicity against LFA-3 and HER2/neu. *Exp Hematol* 27:1533–1541
28. Kawaguchi Y, Kono K, Mizukami Y, Mimura K, Fujii H (2009) Mechanisms of escape from trastuzumab-mediated ADCC in esophageal squamous cell carcinoma: relation to susceptibility to perforin-granzyme. *Anticancer Res* 29:2137–2146
29. Evans MK, Sauer SJ, Nath S, Robinson TJ, Morse MA, Devi GR (2016) X-linked inhibitor of apoptosis protein mediates tumor cell resistance to antibody-dependent cellular cytotoxicity. *Cell Death Dis* 7: e2073. <https://doi.org/10.1038/cddis.2015.412>
30. Mass RD, Press MF, Anderson S, Cobleigh MA, Vogel CL, Dybdal N, Leiberman G, Slamon DJ (2005) Evaluation of clinical outcomes according to HER2 detection by fluorescence in situ hybridization in women with metastatic breast cancer treated with trastuzumab. *Clin Breast Cancer* 6:240–246. <https://doi.org/10.3816/CBC.2005.n.026>
31. Grugan KD, McCabe FL, Kinder M et al (2012) Tumor-associated macrophages promote invasion while retaining Fc-dependent anti-tumor function. *J Immunol* 189:5457–5466. <https://doi.org/10.4049/jimmunol.1201889>
32. Leidi M, Gotti E, Bologna L et al (2009) M2 macrophages phagocytose rituximab-opsonized leukemic targets more efficiently than m1 cells in vitro. *J Immunol* 182:4415–4422. <https://doi.org/10.4049/jimmunol.0713732>
33. van Ravenswaay Claasen HH, Kluin PM, Fleuren GJ (1992) Tumor infiltrating cells in human cancer. On the possible role of CD16<sup>+</sup> macrophages in antitumor cytotoxicity. *Lab Invest* 67: 166–74
34. Beum PV, Mack DA, Pawluczko AW, Lindorfer MA, Taylor RP (2008) Binding of rituximab, trastuzumab, cetuximab, or mAb T101 to cancer cells promotes trogocytosis mediated by THP-1 cells and monocytes. *J Immunol* 181:8120–8132
35. Williams MA, Newland AC, Kelsey SM (1999) The potential for monocyte-mediated immunotherapy during infection and malignancy. Part I: apoptosis induction and cytotoxic mechanisms. *Leuk Lymphoma* 34:1–23. <https://doi.org/10.3109/10428199909083376>
36. Park S, Jiang Z, Mortenson ED et al (2010) The therapeutic effect of anti-HER2/neu antibody depends on both innate and adaptive immunity. *Cancer Cell* 18: 160–70. <https://doi.org/10.1016/j.ccr.2010.06.014>
37. Gennari R, Menard S, Fagnoni F et al (2004) Pilot study of the mechanism of action of preoperative trastuzumab in patients with primary operable breast tumors overexpressing HER2. *Clin Cancer Res* 10:5650–5655. <https://doi.org/10.1158/1078-0432.CCR-04-0225>